ACS Macro Letters

Letter

pubs.acs.org/macroletters

Cylindrical Nanostructure of Rigid-Rod POSS-Containing Polymethacrylate from a Star-Branched Block Copolymer

Raita Goseki,[†] Akira Hirao,[†,‡] Masa-aki Kakimoto,[†] and Teruaki Hayakawa*[,†]

[†]Department of Organic, Polymeric Materials, Tokyo Institute of Technology, 2-12-1-S8-36 O-okayama, Meguro-ku, Tokyo 152-8552, Japan

[‡]Institute of Polymer Science, Engineering, National Taiwan University, No. 1, Sec. 4, Roosevelt Road, Taipei 10617, Taiwan

Supporting Information

ABSTRACT: A nanostructure consisting of rectangular polyhedral oligomeric silsesquioxane (POSS) nanodomains packed into a hexagonal lattice was observed in POSS-containing A_2B star-branched polymers. The A_2B star-branched polymers, which comprised polystyrene (A) and bulky POSS-containing poly(methacrylate) (PMAPOSS) (B) units, were synthesized by anionic polymerization and addition reaction. The self-assembled structures of the A_2B star-branched polymers were studied via transmission electron microscopy (TEM) and small- and wide-angle X-ray scattering (SAXS and WAXS, respectively). It was found that a rectangular nanostructure was packed into a hexagonal arrangement of nanodomains for a PMAPOSS volume fraction of 40 vol. % in the star-branched polymer. In addition, the cylinder-like nanostructure of bulky POSS observed, which is not observed in the case of PS-*b*-PMAPOSS diblock copolymers, was formed owing to the curvature effect, which is the result of the branched architecture of the copolymer.

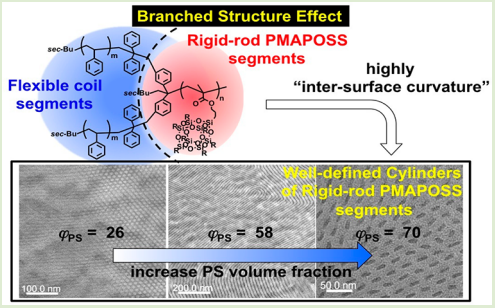

Self-assembled nanostructures with periodic patterns that form in bulk as well as in thin films of block copolymers can be tuned in size, with the sizes ranging from a few nanometers to hundreds of nanometers, by varying the chemical compositions and molecular weights of the copolymers. Thus, significant research efforts have been devoted to fabricated nanostructures with well-defined morphologies from functionalized block copolymers by modifying the chemical components of the copolymers. This has been done to investigate the correlation between the morphologies of the nanostructures and their functionalities.[1−7]

Interest in organic−inorganic hybrid block copolymers has increased in particular because incorporating inorganic materials in polymeric materials can yield novel hybrid materials that exhibit promising characteristic properties not attainable in conventional block copolymers.[8−12] Polyhedral oligomeric silsesquioxanes (POSSs), an inorganic material, have attracted a great deal of attention in the field of material science because of their unique nanoscale cage-shaped structure and high solubility. Therefore, a number of well-defined POSS-containing polymers have been synthesized via recently developed living/controlled polymerization techniques. These polymers display desirable characteristic properties, such as high thermal and mechanical resistance as well as high resistance to oxidation.[13−15] Recently, we had reported the development and self-assembly of a series of POSS-containing polymethacrylate (PMA)-based diblock copolymers (PMA-POSS). We found that a well-defined microphase separated the nanostructures from the bulk. This microphase also existed in the thin film state.[16−22] However, the cylindrical structures that comprise the minor domains of the POSS segments were not observed. This was in spite of the fact that the structures of the microphase-separated PMAPOSS-containing polymers could be varied from sphere-like to lamellae-like by altering the PMAPOSS volume fraction. Thus, morphology control is essential for ensuring that these attractive PMAPOSS-containing block copolymers exhibit desirable properties that make them suitable for use in practical applications.

This type of phase-separation behavior is often observed in the so-called "rod−coil" block copolymers as well.[23−40] The rod segments of these copolymers are commonly based on stiff and bulky molecules such as liquid crystals and π-conjugated polymers, while the coil segments that are commonly employed include polystyrene (PS), poly(isoprene), poly(butadiene), poly(dimethylsiloxane), and polyethylene oxide. The reason the phase-separation behavior of rod−coil block copolymers is different from that of conventional coil−coil block copolymers is that rod−coil block copolymer systems are affected by an additional molecular parameter: there exists a conformational asymmetry between the fully extended rod length and coil radius of gyration, thus it has an impact on the interfacial area of the equilibrium microphase. In addition, interactions such as hydrogen bonding, $\pi-\pi$ interactions, and liquid crystalline interactions also take place between the rod blocks. Indeed,

Received: March 13, 2013
Accepted: July 1, 2013
Published: July 3, 2013

   dx.doi.org/10.1021/mz400125t | *ACS Macro Lett.* 2013, 2, 625−629

since the POSS molecule itself is bulky and crystalline, it may be said that its size causes the distinct phase-separation behavior. Therefore, to decrease this mismatch in the sizes between the bulky-POSS-containing segments and the coil segments, it is even more important to be able to control the morphologies of the PMAPOSS-containing block copolymers.

In this study, we devised a new approach for designing polymer structures to obtain POSS with a cylindrical microphase-separated structure having a volume fraction unobtainable using POSS-containing diblock copolymers. To do so, we employed copolymers with well-defined branched structures such as dendron-linear polymer, dendronized polymer, and star-branched polymer because the branched segments of these copolymers allow for greater curvature at the A−B interface. Although, in the case of dendritic structure, much experiments and theories have been reported, a multistep reaction is needed for preparing sufficient molecular weight compounds.[41−43] However, A_2B star-branched copolymers, the simplest star-branched polymers, have been actually known to be more easily synthesized as sufficient molecular weight polymer by addition reaction between a functionalized polymer and a polymer anion and to exhibit distinctly shifted phase boundaries.[44−52] Therefore, by preparing the star-branched polymers that have the rigid-rod PMAPOSS segments, the curvature of the interfaces became large, and the size mismatch was cancelled.

Herein, we describe the procedure for synthesizing a POSS-containing A_2B star-branched polymer in which PS was the A segment and PMAPOSS was the B segment. The self-assembled structures obtained using PMAPOSS in the A_2B star-branched polymer in various volumetric concentrations were also investigated.

Star-branched PS_2−PMAPOSS was prepared by means of living anionic polymerization using 1,1-bis(3-*tert*-butyldimethylsilyloxymethylphenyl)ethylene (labeled **1** in Scheme 1). The precursor polymer, α-chain-ended *tert*-butyl

Scheme 1. Synthetic Route of Star-Branched PS_2−PMAPOSS

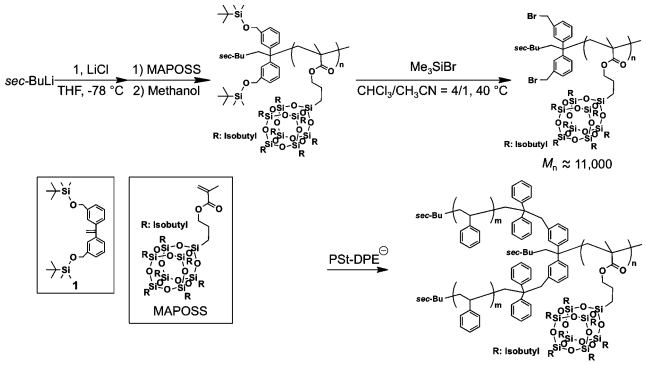

dimethyl silyloxy difunctionalized-PMAPOSS (PMAPOSS-$OTBS_2$), was prepared by anionic polymerization, with the functionalized 1,1-diphenylethylene anions prepared from **1** and *sec*-butyllithium (*sec*-BuLi). Then, PMAPOSS-$OTBS_2$ was made to react with Me_3SiBr to obtain benzyl bromide (BnBr)-difunctionalized PMAPOSS (PMAPOSS-$BnBr_2$), with the BnBr group reacting with the polymer anions.[51,52]

The conversion of PMAPOSS-$OTBS_2$ to PMAPOSS-$BnBr_2$ was quantitatively confirmed by ^1H and ^{29}Si nuclear magnetic resonance (NMR) spectroscopies, with there being no evidence of an undesirable side reaction. In addition, size-exclusion chromatography (SEC) peaks of the polymers, reflecting their shapes and elution counts, were determined both before and after the conversion reaction and were found to be almost similar. As a last step, these polymers were made to react with 1.2−2.0-fold excess for the BnBr reaction site and living PS end-capped with a DPE anion.

The SEC chromatograms of the polymers after the linking reaction displayed two distinct sharp peaks: one corresponding to the target-linked polymer and the other to the excess, unreacted PS anions (Figure S1, Supporting Information). No signal was detected in the high-molecular-weight region, indicating the other side reaction did not take place under the reaction conditions. The target polymer was isolated by fractional precipitation using acetone (when the number average molecular mass (M_n) of the unreacted PS was less than 30k) or SEC fractionation (when the M_n of the excess PS was greater than 30k). The chemical structures of the star-branched PS_2−PMAPOSS polymers were determined using ^1H, ^{13}C, and ^{29}Si NMR spectroscopy and infrared (IR) spectroscopy. In addition, their molecular weights and molecular weight distributions were measured using SEC.

The ^1H NMR spectrum of the star-branched PS_2−PMAPOSSs showed clearly the successful incorporation of each block. This was indicated by the appearance of methylene (-OSiCH_2) protons corresponding to PMAPOSS at 0.60 ppm and PS aromatic protons at 7.06−6.36 ppm (Figure S2, Supporting Information). The molecular weight distributions, obtained via SEC-based analysis, were narrow (below 1.08). The results of the polymerization process were listed in Table 1. Hence, the compositions of the star-branched PS_2−PMAPOSSs could be ascertained by using the integration ratios from the ^1H NMR spectra of the aromatic protons of PS and comparing them with the integrated intensities of the signals corresponding to the methylene protons of PMAPOSS, along with the M_n values. The volume fraction of each block was estimated from the density of PS (1.05 g cm^{-3}) and that of PMAPOSS[17] (1.14 g cm^{-3}) in combination with the ^1H NMR data.

The five different star-branched PS_2−PMAPOSSs investigated in the present study had overall PS-to-PMAPOSS volume fractions ranging from 26 to 70 vol %. In the case of a coil−coil diblock copolymer, this would lead to the separation of the microphase into cylinder-like, lamellar-like, and inverse cylinder-like structures.

The morphologies of the samples were characterized using small-angle X-ray scattering (SAXS), wide-angle X-ray scattering (WAXS), and transmission electron microscopy (TEM), which were performed on samples subjected to thermal annealing to reach thermodynamic equilibrium; the polymers were annealed at 180 °C for 24 or 48 h in a vacuum oven. This temperature was necessary to erase the thermal histories of the samples and to keep the polymer blends within the temperature range of 100 °C (the glass transition temperature of PS) and 180 °C (the melting point of PMAPOSS).

Figure 1 showed the SAXS profiles and TEM images of the star-branched PS_2−PMAPOSSs. The profile of the star-branched PS_2−PMAPOSS **1** (containing 26 vol % PS) exhibited three scattering peaks, with the relative position ratios of the peaks being $1:3^{1/2}:4^{1/2}$. Using the position of the first-order peak (2θ = 0.55), the long-period spacing of the cylinder-like structure was found to be equal to 18.5 nm. For increases in the volume fraction of PS to 42 and 58 vol %, the

dx.doi.org/10.1021/mz400125t | ACS Macro Lett. 2013, 2, 625−629

Table 1. Polymerization Results of Star-Branched PS_2−PMAPOSSs

polymers	PS M_n[a]	PMAPOSS M_n[a]	total M_n[a]	M_w/M_n[a]	wt % PS[b]	vol % PS[c]	morphology[d]
PS_2−PMAPOSS **1**	5100	10500	21800	1.06	24	26	PS cylinder
PS_2−PMAPOSS **2**	20600	10500	35400	1.08	40	42	lamella
PS_2−PMAPOSS **3**	23400	11200	39800	1.04	54	58	lamella
PS_2−PMAPOSS **4**	29600	10500	66300	1.02	60	63	POSS cylinder
PS_2−PMAPOSS **5**	39200	11200	78500	1.04	67	70	POSS cylinder
PS_{266}-*b*-$PMAPOSS_{20}$[e]	26600	19000	47000	1.05	59	63	lamella

[a]Estimated by SEC with standard polystyrene samples. [b]Determined by ^{1}H NMR results and molecular weights. [c]Estimated by using the PS density of 1.05 g/cm^3 and the PMAPOSS density of 1.14 g/cm^3 in combination with the ^{1}H NMR data. [d]Determined by SAXS and TEM results. [e]Ref 17.

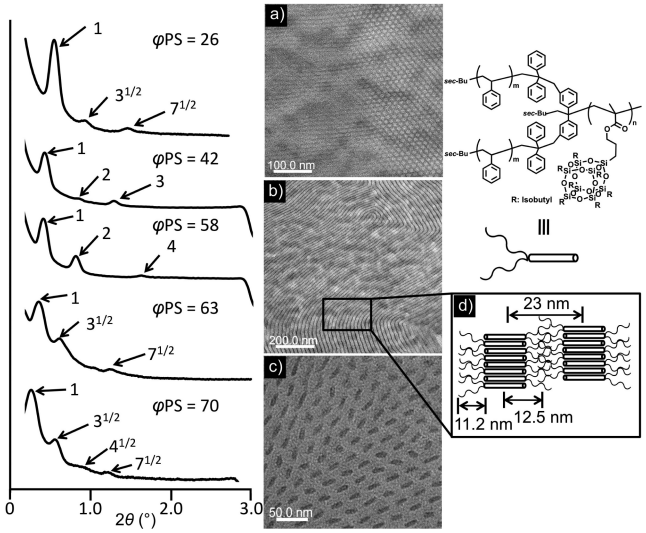

Figure 1. SAXS profiles and TEM images of star-branched PS_2−PMAPOSSs annealed at 180 °C. (a) PS_2−PMAPOSS **1** (PS-cylinder), for 24 h, (b) PS_2−PMAPOSS **3** (lamella), for 24 h, (c) PS_2−PMAPOSS **5** (POSS-cylinder), for 48 h, and (d) schematic illustration of lamellae-like nanostructure.

SAXS diffraction profiles exhibited three addition reflections, whose position ratios were 1:2:3, indicating the star-branched polymers **2** and **3** formed a lamellar structure with the *d*-spacing being 21 and 23 nm, respectively. In contrast, for higher PS volume fractions (63 and 70 vol %), the SAXS patterns showed higher-order peaks at $1:3^{1/2}:7^{1/2}$ and $1:3^{1/2}:4^{1/2}:7^{1/2}$. This indicated that cylinder and/or spherical phases were formed with the *d*-spacing being 29 and 38 nm, respectively. In addition, TEM was employed to support the findings of the SAXS-based analysis and explore the self-assembled star-shaped PS_2−PMAPOSSs nanostructures in real space.

All the polymers investigated exhibited well-defined morphologies, which resulted from the microphase separation. All the samples imaged using TEM were imaged without staining, as the mass of the POSS-containing segment, which was higher than that of the PS segment, could result in the PMAPOSS domains appearing dark and the PS domains appearing bright. The TEM images of the star-branched PS_2−PMAPOSSs **1** and **3** are shown in Figures 1 (a) and (b), respectively, along with the corresponding SAXS profiles. By directly measuring the distances between the center-to-center PS domains on the images, it was found that the measured distances were almost the same as the long-period spacing as determined by SAXS (Figure 1a). On the other hand, in the case of the high-coil-fraction star-branched PS_2−PMAPOSS **5** (φ_{PS} = 70 vol %), self-assembly into hexagonal structures, the type not seen in the case of PS-*b*-PMAPOSS diblock copolymers with similar volume fractions, was observed (Figure 1(c)).

An interesting comparison can be made between the diblock copolymer PS_{266}-*b*-$PMAPOSS_{20}$ (ref 17) and the star-branched PS_2−PMAPOSS **4** (Figure 2). These samples contain the PS component in almost the same volume fractions (φ_{PS} = 63 vol %), and yet they exhibited very different morphologies. In the case of the PMAPOSS-containing star-branched polymer, it was found that the simultaneous control of the volume fraction and the microphase behavior was possible by changing the molecular architecture. It was also found that the volume fraction of PS required for the formation of cylinder-like nanostructures was about 60 vol %. Since each PMAPOSS arm is attached to two PS arms for the star-branched polymers, as opposed to just one for a linear diblock, there will be more crowding on the PS side of the interface. As a result, this will favor a higher degree of curvature, and it causes the difference in the microphase structures (Figure 2). It could be seen that, unlike the usually formed nanostructures, which are rectangular, this structure was cylindrical, with the nanodomain boundaries being 12.0 nm wide and 5.4 nm thick. On the basis of the results of a simulation of the microphase separation of a rod−coil diblock copolymer, it was found that this ellipsoidal cylinder-like nanostructure had a higher free energy than that of a more rounded structure and was also less stable. However, such a structure is often observed in the case of rod−coil diblock copolymers.[35−40] It should also be mentioned that the

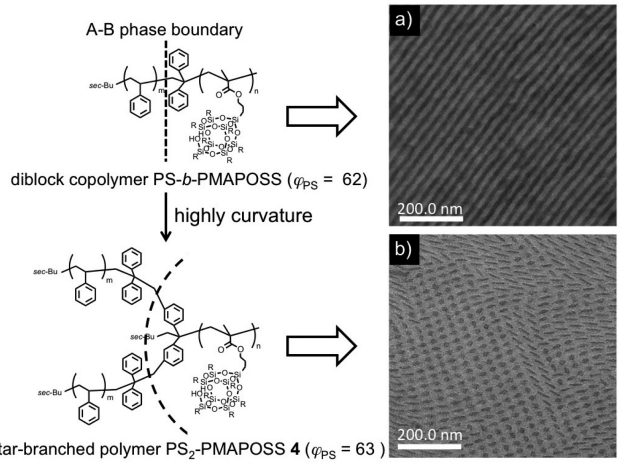

Figure 2. Differences between the morphology of (a) linear PS-*b*-PMAPOSS (that was synthesized and measured according to ref 17) and (b) the star-branched PS_2−PMAPOSS **4**. The greater crowding on the PS side of the interface for the star-branched polymer case leads to a high degree of curvature.

dx.doi.org/10.1021/mz400125t | *ACS Macro Lett.* 2013, 2, 625−629

ellipsoidal cylinder-like structures were distinctly observed in the current study.

Next, to determine which model more suitably described the observed structure, the lengths of the PMAPOSS rods were estimated. Since the *d*-spacing depends on the total molecular weight of the polymer, the relations between the molecular weight per PS chain and the resulting *d*-spacing values of the star-branched PS_2−PMAPOSSs were plotted (Figure S4, Supporting Information). There existed proportionality between the two, and using a linear fit that passed through the origin resulted in a *y*-axis intercept of 117.9 Å, which was reflective of the length of the PMAPOSS segment. Using the molecular weights of the polymers, determined via SEC, and the molecular weight of the monomer, the number of MAPOSS units in the polymer was calculated and found to be about 10 units. POSS molecules are known to have shapes similar to those of nanosized cages, with the size of the cage being 1.2 nm in dimension. Therefore, the calculated values of the number of units present and the cage size were in good agreement with the estimated PMAPOSS length. Thus, we concluded that the PMAPOSS length is 11.8 nm.

On the basis of the above results, it was considered how lamellar structure would be formed of star-branched PS_2−PMAPOSS. In general, the results of attempts to increase the size of the lamellar domain of rod−coil block copolymers by varying the molecular weight blocks were significantly different from those observed in the case of coil−coil block copolymers. In the case of coil−coil diblock copolymers, as the molecular weight of the blocks is increased, the coils become free to expand three-dimensionally, and scaling increases by a factor of $N^{2/3}$, where N is the number of volumetric repeat units. In contrast, for a rod−coil block copolymer with a static rod segment of length a, coil fraction φ, and a specified rod orientation θ relative to the lamellar normal, the width of the rod nanodomain should be equal to the rod length in the direction of the lamellar normal, $Na(1 - \varphi)\cos\theta$. From this theory and the above-mentioned calculation results, it was thought that the rod segments were thus expanded without tilting. On the other hand, the PS length was estimated from the *d*-spacing of the lamella and found to be 11.2 nm. The theoretical expanded PS chain length was found to be 10 nm, which was calculated using the static length (0.434 $Å^2$ $mol\ g^{-1}$) and the molecular weight of PS.[53] Thus, the estimated distance was longer than the theoretical value. Therefore, as shown in Figure 1d, it was assumed that the PS and the PMAPOSS chains were both in the extended state and that the PS chains were interwoven in the lamellar structure.

By increasing the PS volume fraction to 63 vol %, lateral interactions between the POSSs along the PS direction were disrupted owing to the bulk steric hindrance of the long PS chains. As a result, the microphase-separated structures of star-branched PS_2−PMAPOSSs **4** and **5** were switched from the lamellar phase to a more stable rectangular cylinder. In the rod−coil diblock copolymer, cylindrical structure is considered since the rod segments assembled into a interdigitated bilayer, a monolayer, or hockey puck arrangement.[29,30,32] The length of the rectangular nanodomain in the TEM image was almost equal to the length of the extended PMAPOSS segments. Similar results have been reported by L. H. Radzilowski et al., and it was thus assumed that the cylinder-like structure might constitute the interdigitated bilayers of rods.[29] However, a more detailed analysis of the rectangular nanodomain is underway, and its results will be described in a future report.

Finally, to determine whether the POSS cages were organized within the self-assembled nanostructure, WAXS-based measurements were performed (Figure 3). The

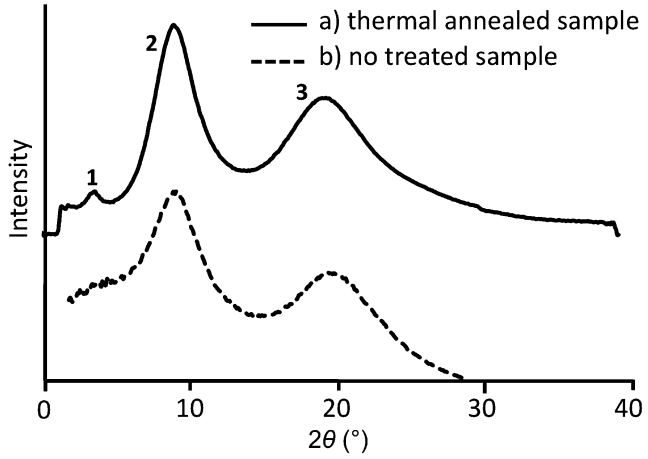

Figure 3. WAXS profiles of star-branched PS_2−PMAPOSS **5**: (a) thermal annealed sample (solid line) and (b) no treated sample (dot line).

unannealed star-branched PS_2−PMAPOSS polymer exhibited two diffraction peaks, at $2\theta = 8.56$ and 18.4° (labeled **2** and **3** in Figure 3), respectively, which corresponded to *d*-spacing values of 1.02 and 0.47 nm. In the case of the annealed sample, however, an additional diffraction peak, at $2\theta = 3.52°$ (labeled **1** in Figure 3), corresponding to a *d*-spacing of 2.5 nm, emerged. This indicated the aggregation of the POSS units. On the basis of the results of our previous study, these lengths were attributable to the average distance between the main chains of PMAPOSS (2.5 nm), the average distance between the POSS cage in the PMAPOSS block (1.0 nm), and the π−π interaction of the PS block (0.47 nm), respectively. A characteristic reflection peak **1**, which corresponded to a periodic length of 2.5 nm, was also seen in the case of the thermally annealed sample.[17,19] This indicated that the thermal annealing induced the molecular stacking of the PMAPOSS layers and the aggregation of the formed POSS crystalline simultaneously. Thus, the aggregation and crystallization of POSS were observed in the PMAPOSS segments that were cylinder-like in structure.

To summarize, we synthesized star-branched PS_2−PMAPOSSs and studied their nanostructures and self-assembly mechanisms. Well-defined PS_2−PMAPOSS star-branched polymers were synthesized by living anionic polymerization and an addition reaction. We also determined that a PMAPOSS-containing block copolymer could be made to self-assemble into cylinder-like nanostructures by using an architectural approach. Thus, the results of this study can aid in the application of rod−coil block copolymers in various areas since it has been shown that it is possible to control the structures of such copolymers.

■ ASSOCIATED CONTENT

Ⓢ Supporting Information

Experimental section and ^1H NMR spectra, SEC curves, and TEM images of the synthesized star-branched polymers (Figures S1−4). This material is available free of charge via the Internet at http://pubs.acs.org.

dx.doi.org/10.1021/mz400125t | *ACS Macro Lett.* 2013, 2, 625−629

AUTHOR INFORMATION

Corresponding Author

*E-mail: hayakawa.t.ac@m.titech.ac.jp.

Notes

The authors declare no competing financial interest.

ACKNOWLEDGMENTS

We also thank Ryohei Kikuchi University Corporation Tokyo Institute of Technology Center for Ascended Materials Analysis, for the measurement of TEM.

REFERENCES

(1) Lazzari, M.; Lopez-Quintela, M. A. *Adv. Mater.* **2003**, *15*, 1583.
(2) Park, C.; Yonn, J.; Thomas, E. L. *Polymer* **2003**, *44*, 6725.
(3) Cheng, J. Y.; Ross, C. A.; Smith, H. I.; Thomas, E. L. *Adv. Mater.* **2006**, *18*, 2505.
(4) Bang, J.; Jeong, U.; Ryu, D. Y.; Russell, T. P.; Hawker, C. J. *Adv. Mater.* **2009**, *21*, 4769.
(5) Lee, D. H.; Shin, D. O.; Lee, W. J.; Kim, S. O. *Adv. Mater.* **2008**, *20*, 2480.
(6) Rzayev, J.; Hillmyer, M. A. *Macromolecules* **2005**, *38*, 3.
(7) Liu, C.-L.; Lin, C.-H.; Kuo, C.-C.; Lin, S.-T.; Chen, W.-C. *Prog. Polym. Sci.* **2011**, *36*, 603.
(8) Nguyan, P.; Gomez-Elipe, P.; Manners, I. *Chem. Rev.* **1999**, *99* (6), 1515.
(9) Manners, I. *J. Polym. Sci., Part A: Polym. Chem.* **2002**, *40*, 179.
(10) Choi, H., K.; Gwyther, J.; Manners, I.; Ross, C. A. *ACS Nano* **2012**, *6*, 8342.
(11) Lu, J. Q.; Rider, D. A.; Onyegam, E.; Wang, H.; Winnik, M. A.; Manners, I.; Cheng, Q.; Fu, Q.; Liu, J. *Langmuir* **2006**, *22*, 5174.
(12) Wang, H.; Wang, X.; Winnik, M. A.; Manners, I. *J. Am. Chem. Soc.* **2008**, *130*, 12921.
(13) Cordes, D. B.; Lickiss, P. D.; Rataboul, F. *Chem. Rev.* **2010**, *110*, 2081.
(14) Wu, J.; Mather, P. T. J. *Macromol. Sci., Part C: Polym. Rev.* **2009**, *49*, 25.
(15) Kuo, S.-W.; Chang, F.-C. *Prog. Polym. Sci.* **2011**, *36*, 1649.
(16) Hirai, T.; Leolukman, M.; Liu, C. C.; Han, E.; Kim, Y. J.; Ishida, Y.; Hayakawa, T.; Kakimoto, M.; Nealey, P. F.; Gopalan, P. *Adv. Mater.* **2009**, *21*, 4334.
(17) Hirai, T.; Leolukman, M.; Jin, S.; Goseki, R.; Ishida, Y.; Kakimoto, M.; Hayakawa, T.; Ree, M.; Gopalan, P. *Macromolecules* **2009**, *42*, 8835.
(18) Ishida, Y.; Tada, Y.; Hirai, T.; Goseki, R.; Kakimoto, M.; Yoshida, H.; Hayakawa, T. *J. Photopolym. Sci. Technol.* **2010**, *23*, 155–159.
(19) Ahn, B.; Hirai, T.; Jin, S.; Rho, Y.; Kim, K.-W.; Kakimoto, M.; Gopalan, P.; Hayakawa, T.; Ree, M. *Macromolecules* **2010**, *43*, 10568.
(20) Ishida, Y.; Hirai, T.; Goseki, R.; Tokita, M.; Kakimoto, M.; Hayakawa, T. *J. Poly. Sci., Part A: Polym. Chem.* **2011**, *49*, 2653.
(21) Goseki, R.; Hirai, T.; Ishida, Y.; Kakimoto, M.; Hayakawa, T. *Polym. J.* **2012**, *44*, 658.
(22) Tada, Y.; Yoshida, H.; Ishida, Y.; Hirai, T.; Bosworth, J. K.; Dobisz, E.; Ruiz, R.; Takenaka, M.; Hayakawa, T.; Hasegawa, H. *Macromolecules* **2012**, *45*, 292.
(23) Chang, C.-J.; Lee, Y.-H.; Chen, H.-L.; Chaing, C.-H.; Hsu, H.-F.; Ho, C.-C.; Su, W.-F.; Dai, C.-A. *Soft Matter* **2011**, *7*, 10951.
(24) Li, C. Y.; Tenneti, K. K.; Zhang, D.; Zhang, H.; Wan, X.; Chen, E.-Q.; Zhou, Q.-F.; Carlos, A.-O.; Igos, S.; Hsiao, B. S. *Macromolecules* **2004**, *37*, 2854.
(25) Tenneti, K. K.; Chen, X.; Li, C. Y.; Tu, Y.; Wan, X.; Zhou, Q.-F.; Sics, I.; Hsiao, B. S. *J. Am. Chem. Soc.* **2005**, *127*, 15481.
(26) Tenneti, K. K.; Chen, X.; Li, C. Y.; Shen, Z.; Wan, X.; Fan, X.; Zhou, Q.-F.; Rong, L.; Hsiao, B. S. *Macromolecules* **2009**, *42*, 3510.
(27) Olsen, B. D.; Shah, M.; Ganesan, V.; Segalman, R. A. *Macromolecules* **2008**, *41*, 6809.
(28) Hillmyer, M. A.; Lodge, T. P. *J. Polym. Sci., Part A: Polym. Chem.* **2002**, *40*, 1.
(29) Radzilowski, L. H.; Carragher, B. O.; Stupp, S. I. *Macromolecules* **1997**, *30*, 2110.
(30) Radzilowski, L. H.; Stupp, S. I. *Macromolecules* **1994**, *27*, 7747.
(31) Müller, M.; Schick, M. *Macromolecules* **1996**, *29*, 8900.
(32) Williams, D. R. M.; Fredrickson, G. H. *Macromolecules* **1992**, *25*, 3561.
(33) Li, W.; Gersappe, D. *Macromolecules* **2001**, *34*, 6783.
(34) Ryu, J.-H.; Oh, N.-K.; Zin, W.-C.; Lee, M. *J. Am. Chem. Soc.* **2004**, *126*, 3551.
(35) Lee, Y.-H.; Yen, W.-C.; Su, W.-F.; Dai, C.-A. *Soft Matter* **2011**, *7*, 10429.
(36) Olsen, B. D.; Segalman, R. A. *Macromolecules* **2007**, *40*, 6922.
(37) Sary, N.; Brochon, C.; Hadziioannou, G.; Mezzenga, R. *Eur. Phys. J. E* **2007**, *24*, 379.
(38) Sary, N.; Rubatat, L.; Brochon, C.; Hadziioannou, G.; Roukolainen, J.; Mezzenga, R. *Macromolecules* **2007**, *40*, 6990.
(39) Ho, C.-C.; Lee, Y.-H.; Dai, C.-A.; Segalman, R. A.; Su, W.-F. *Macromolecules* **2009**, *42*, 4208.
(40) Bu, L.; Qu, Y.; Yan, D.; Geng, Y.; Wang, F. *Macromolecules* **2009**, *42*, 1580.
(41) Lee, W. B.; Elliott, R.; Mezzenga, R.; Fredrickson, G. H. *Macromolecules* **2009**, *42*, 849.
(42) Mezzenga, R.; Ruokolainen, J.; Canilho, N.; Kasëmi, E.; Schlüter, D. A.; Lee, W. B.; Fredrickson, G. H. *Soft Matter* **2009**, *5*, 92.
(43) Merlet-Lacroix, N.; Rao, J.; Zhang, A.; Schlüter, D. A.; Bolisetty, S.; Ruokolainen, J.; Mezzenga, R. *Macromolecules* **2010**, *43*, 4752.
(44) Hadjichristidis, N.; Iatrou, H.; Behal, S. K.; Chludzinski, J. J.; Disko, M. M.; Garner, R. T.; Liang, K. S.; Lohse, D. J.; Milner, S. T. *Macromolecules* **1993**, *26*, 5812.
(45) Milner, S. T. *Macromolecules* **1994**, *27*, 2333.
(46) Tselikas, Y.; Iatrou, H.; Hadjichristidis, N.; Liang, K. S.; Mohanty, K.; Lohse, D. J. *J. Chem. Phys.* **1996**, *105*, 2456.
(47) Junnila, S.; Houbenov, N.; Karatzas, A.; Hadjichristidis, N.; Hirao, A.; Iatrou, H.; Ikkala, O. *Macromolecules* **2012**, *45*, 2850.
(48) Shi, Z.; Chen, D.; Lu, H.; Wu, B.; Ma, J.; Cheng, R.; Fang, J.; Chen, X. *Soft Matter* **2012**, *8*, 6174.
(49) Canilho, N.; Kasëmi, E.; Schlüter, A. D.; Ruokolainen, J.; Mezzenga, R. *Macromolecules* **2007**, *40*, 7609.
(50) Cai, H.; Jiang, G.; Shen, Z.; Fan, X. *Macromolecules* **2012**, *45*, 6176.
(51) Hirao, A.; Matsuo, A. *Macromolecules* **2003**, *36*, 9742.
(52) Haraguchi, N.; Hirao, A. *Macromolecules* **2003**, *36*, 9364.
(53) Fetters, L. J.; Lohse, D. J.; Richter, D.; Witten, T. A.; Zirkel, A. *Macromolecules* **1994**, *27*, 4639.